Research Article

Journal of Environmental Nanotechnology

Fabrication and Characterization of Corn Starch-blended Polyhydroxybutyrate Films

S. Venkatesh and Vijayalakshmi Shankar*

CO_2 Research and Green Technologies Centre, Vellore Institute of Technology, Vellore, TN, India

Received: 05.07.2025 Accepted: 13.08.2025 Published: 30.09.2025

*vijimicro21@gmail.com

ABSTRACT

Polyhydroxybutyrate (PHB) is a biodegradable polyester from natural resources commonly applied in food packaging due to its fast biodegradation. This study investigates PHB as a primary matrix with corn starch as a supplementary reinforcement. Traditional casting method was used with different weight ratios of PHB and corn starch (50/50, 60/40, and 70/30). Mechanical properties, morphological characteristics and structural analyses were evaluated using Fourier transform infrared spectrometry (FTIR), scanning electron microscopy (SEM), and X-ray diffraction (XRD) techniques. A field emission scanning electron microscope (FESEM) with energy-dispersive spectroscopy (EDS) was employed to study biodegradation in the PHB-corn starch combinations. The SEM images revealed that corn starch is uniformly dispersed within the PHB matrix, particularly in the 50/50 and 70/30 ratios, while the 60/40 ratio showed pore formation due to poor dispersion. Similarly, FTIR indicated that no interfacial intermetallics were present in the PHB-corn starch blends at the 60/40 ratio, which also displayed lower tensile strength compared to the other two blends, attributed to particulate agglomeration. Soil burial tests revealed that the optimal proportion of PHB:Corn starch is 70:30.

Keywords: Polyhydroxybutyrate; Corn starch blends; Biodegradable films; Mechanical properties; Soil burial test.

1. INTRODUCTION

Every decade, an increase in plastic waste is generated, while the timeline for biodegradation remains unclear (Plavec *et al.* 2020). Growing environmental awareness has inspired the creation of new biodegradable materials, especially for single-use plastics (Lee *et al.* 2021). People encounter plastic in everyday applications, including household items, construction, packaging, medical uses, and automotive sectors (Lin *et al.* 2021). Furthermore, global plastic production exceeds 340 million tons, with projections indicating continued growth in the upcoming years. Plastics are primarily produced from petroleum by-products, significantly contributing to greenhouse gas emissions throughout their lifecycle (Song *et al.* 2013). If the demand for plastics surges, global emissions could reach 6.5 gigatons of carbon dioxide by 2050. Consequently, reducing reliance on fossil-based plastics is essential in favour of more sustainable alternatives (Saratale *et al.* 2021). In addition to recycling plastic, leveraging renewable energy to produce bio-based polymers is a viable alternative to traditional plastics. Indeed, bio-based plastics could meet up to 70% of plastic demands, potentially preventing 300 million tons of carbon dioxide emissions. Imagining a world without polymers is impractical in today's context (Moreira *et al.* 2022).

Polymers are a key aspect of day-to-day life due to their appropriate properties, ease of processing, ecological resistance to corrosion and chemicals, and reasonable cost compared to traditional materials (Nygaard *et al.* 2021). Plastics play a significant role in various applications such as water purification, packaging, aeronautics, biomedical, and automotive sectors (Park *et al.* 2021). Even though their mechanical attributes are notable, traditional non-biodegradable polymers are not eco-friendly. Nowadays, the usage and synthesis of biodegradable polymers are increasing. Primarily, the first generation of bio-based biodegradable polyester, commonly known as polylactic acid (PLA), is extensively utilised. This source is naturally extracted from sugar and corn starch (Zhang *et al.* 2020). There are two optical isomeric forms, dextrorotary and laevorotary, which are the monomers of polylactic acid. These polylactic acid polymers are widely used in biomedical and packaging applications due to their renewable and biocompatible properties (Boura *et al.* 2022).

In applications related to food packaging, PLA often requires modification due to its brittle and rigid properties (Fernández *et al.* 2022). Various green polymers, such as chitosan, polybutylene succinate, and starch, are blended with PLA to improve their mechanical properties for biomedical and food packaging use (Briassoulis *et al.* 2022). However, the processing methods for creating PLA with biodegradable polymers are complex, and the mechanical properties are significantly inferior compared to polyhydroxyalkanoates (PHAs). These are a new

generation of polymers that have gained interest in medicine, agriculture, and marine applications (Sirohi 2021). The excessive carbon sources and unwanted growth limits from various microorganisms can reduce the material's effectiveness (Briassoulis *et al.* 2021). Elastomers and thermoplastics are synthetic materials similar to PHAs, with synthetic rubber produced from polypropylene. However, the disposal of these products is complicated, as they require anaerobic conditions for complete degradation into CO_2 and H_2O under various ecological settings such as sewage, seas, lakes, and soils (Sirohi *et al.* 2020).

However, the cost of polyester-based polymers hinders their widespread industrial use. Thus, combining polymeric compounds with two or more base materials offers a more economical alternative for reducing the overall product cost, representing a significant strategy for developing new materials with desired properties (Zoghbi *et al.* 2023). Compared to PLA and PHAs, these alternatives exhibit certain drawbacks and high manufacturing cost, as previously mentioned. Poly (3-hydroxybutyrate), or PHB, is a preferred choice among researchers due to its high crystallinity and melting temperature (Tian *et al.* 2022). Although PHB is thermoplastic and biodegradable, it tends to be brittle when combined with a homopolymer, limiting its applications (Feng *et al.* 2023). Numerous studies have explored this topic, especially regarding PHB blends with biodegradable polymers such as polysaccharides, poly (ε-caprolactone), and poly (vinyl alcohol) (Movahedi and Karbasi, 2022; Asl *et al.* 2022).

Typically, PLA exhibits lower crystallinity, whereas PHB addresses these shortcomings, thereby improving the barrier properties of polylactic acid, which is essential for food packaging applications (Asl *et al.* 2021). Generally, PHB is more biodegradable under typical conditions than PLA (Corradini *et al.* 2011). Some studies underscore PHB's role in enhancing mechanical properties (Ma *et al.* 2014). Kervran *et al.* (2022) reviewed the thermal degradation of PHB and PLA-based polymers and analysed their blending parameters and mechanical characteristics. Compared to PLA, PHB-based biopolymers achieve optimal thermal stability, particularly when reinforced with starch. Nygaard *et al.* (2021) explored the fermentation of PHB to produce biopolymers from fructose materials. Shaken flask cultures produced PHB influenced by Necator type C, leading to improved fermentation methods. Reis *et al.* (2008) prepared PHBs modified with maize starch by increasing weight proportions *via* casting. The resulting PHBs integrated with starch were observed as a heterogeneous dispersion through SEM analysis. Florez *et al.* (2019) examined the effect of PHB as a reinforcing agent in corn starch using compression moulding. Increasing the PHB content and incorporating 35% glycerol enhanced the PHB surface through a plasma treatment. s

However, a rise in the PHB weight percentage resulted in downgraded mechanical properties, negatively affecting interfacial bonding. It is evident from the literature that PHB significantly contributes to biodegradable products, particularly with starch-based reinforcement that enhances mechanical properties. This research employs different volume fractions of PHB (extracted from *Chlorella vulgaris*) and corn starch to fabricate biopolymers using conventional casting techniques.

2. MATERIALS AND METHODS

2.1 Sample Collection

Water samples containing the microalgae *Chlorella vulgaris* are collected from Tiruparankundram Pond, Vandiyur Pond, Vilangudi Pond, and Sellur Pond, Madurai, Tamil Nadu, India. The samples were collected from both top and bottom sections. Each collected sample predominantly contained visible microalgal populations. The samples were stored in sterilised 50-mL tubes, quickly refrigerated, and then transported to the laboratory for further analysis. This sampling method was employed primarily to isolate the microalgal strains producing the highest PHB.

2.1.1 Isolation and Screening of Microalgal Strains

The microalgal species was sterilised and extracted from diverse sources using essential microbial techniques, which included continuous dilution, spread plating, and quadrant streaking on Bold's Basal Medium (BBM) agar plates. The algal culture grown in the laboratory from each set of water samples underwent dilutions ranging from 10^2 to 10^6 times. After dilution, the Petri plates were maintained at a controlled temperature, and morphological identification was carried out using microscopes.

2.1.2 Micro Algal Genomic DNA Isolation and PCR Analysis

Genomic DNA was extracted from robust cultures of selective microalgae using the QIAGEN DNA isolation kit (Qiagen), dissolved in 100 µL of elution buffer (10 mM/L Tris-HCl, pH 8.5), and quantified by measuring the optical density at 260 nm. Polymerase chain reaction amplification was performed with 50 µL reaction mixtures containing 100 ng of template DNA, 20 µmol of 18S rRNA primers, 200 µM of dNTPs, 1.5 mM of $MgCl_2$, 1 U of Taq DNA polymerase (MBI Fermentas), and 10 µL of 10x Taq polymerase buffer. The application process for the 18S rRNA primers is outlined as follows.

18Sf: (5'-CCTGGTTGATCCTGCCAG-3')

18Sr:(5′-TTGATCCTTCTGCAGGTTCA-3')

The amplification started with an initial denaturation at 94°C for 5 minutes, followed by 30 cycles including denaturation at 94°Cfor 1 minute, annealing at 55°C for 1 minute and extension at 72°C for 2 minutes, culminating in a final extension at 72°C for 4 minutes using a thermocycler (iCycler; Bio-Rad Laboratories, CA). The PCR products were assessed on a 1.5% agarose gel for 18S rRNA amplicons in 1x TBE buffer at 100 V. The resulting amplified product was analysed using the ABI PRISM 3730 Genetic Analyser (Applied Biosystems).

2.2 Quantification of PHB

About 0.01 g of PHB was dissolved in 10 mL of chloroform using a water bath set to 65-70°C until the solution becomes clear. This process yielded a 1 mg/ mL PHB stock solution. Then, 1 mL of the 1 mg/ mL stock solution was added to 9 ml of chloroform in a clean tube to get a 100 µg/mL PHB stock solution. This was vortexed and maintained at 65–70 °C. Polyhydroxybutyrate was converted to crotonic acid by acid hydrolysis using 10 mL of conc. sulphuric acid. Formation of crotonic acid was confirmed by recording UV-Vis spectrum at 235 nm. The standard curve was plotted by measuring absorbance at 235 nm against the weight of PHB.

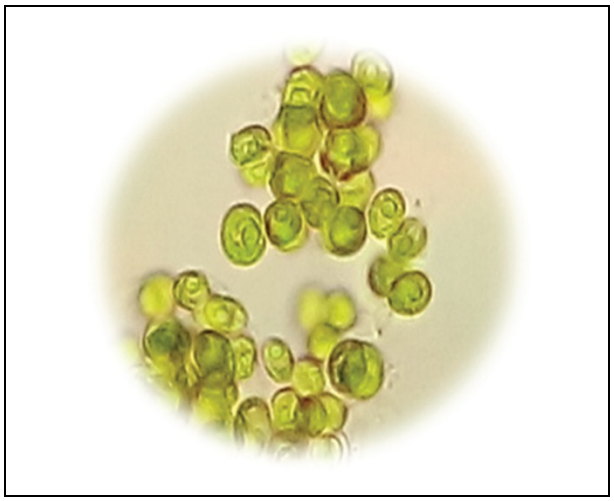


Fig. 1: Microscopic image of *Chlorella vulgaris*

2.3 PHB Extraction Technique

A 100-mL sample was centrifuged at 10,000 rpm for 15 minutes. The supernatant was discarded, and the remaining liquid was treated with 10 mL of sodium hypochlorite, followed by incubation at 30°C for 2 hours. After incubation, the mixture was centrifuged at 5000 rpm for 15 minutes, then washed with methanol and distilled water sequentially. The solution was then dissolved in 5 mL of boiling chloroform, which was concentrated to a minimal volume. Cold methanol was added, and the mixture was refrigerated overnight to precipitate PHB, which was collected through centrifugation.

2.4 Blending of PHB and Corn Starch

Traditional solution casting method was used to blend commercial corn starch with the microalgal PHB to form PHB films. Microalgal PHB and corn starch were mixed in proportions of 50/50, 60/40, and 70/30 using 5% chloroform. Each mixture was kept at 60°C for one hour and stirred continuously on a magnetic stirrer. The thin films were formed by pouring the solution onto a Petri dish as the casting surface. Solvent evaporation occurred overnight on the flat surface at room temperature.

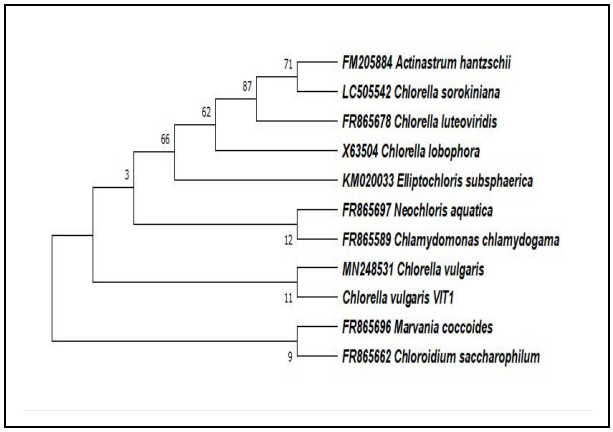


Fig. 2: Sequence Accession Number: OP811012

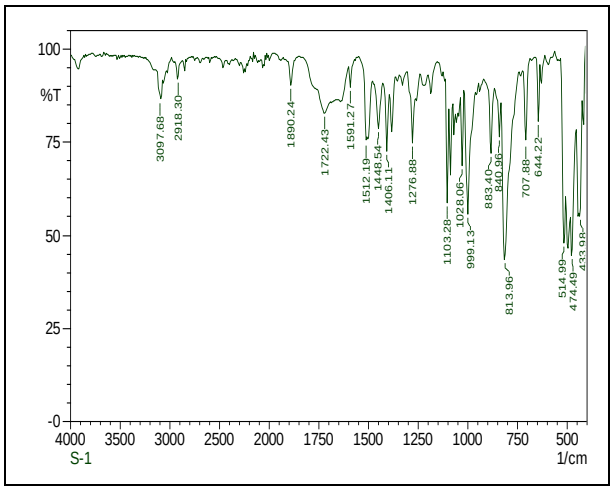


Fig. 3: FTIR spectrum in the zones of PHB (50%) and starch (50%) composite blends

2.5 Characterization Studies

2.5.1 SEM

A JEOL JSM-5410 (Japan) scanning electron microscope was used for the microstructural analysis of the films. The film samples were stored in P_2O_5 for two

weeks to ensure their dryness (theoretical relative humidity in the desiccator is 0). Each film was then frozen in liquid nitrogen and cryo-fractured to examine the surface and cross-section. The films were mounted on gold-coated copper stubs and analysed using an accelerating voltage of 10 kV.

2.5.2 XRD

A Bruker AXS/D8 Advance X-ray diffractometer was used to record X-ray diffraction patterns. Samples were examined within the 2θ range 5º to 50º, utilising Kα Cu radiation (λ: 1.542 Å) at 40 kV and 40 mA, with a step size of 0.05º. Before storage, samples were prepared in 4 cm^2 dimensions to avoid damage. The analysis used the Span 40 and Span 60 reagents.

2.6 Mechanical Characteristics

ASTM D412 was used to assess the moldable characteristics and plasticizingabilities of the samples using the Zwick/Roell Tensile Testing Machine (model Z010).

3. RESULTS AND DISCUSSION

3.1 Identification of Algae

3.1.1 Morphological properties

The initial identification and purity of green microalgal strains with high PHB-content were assessed by fluorescent microscopy (Fig. 1).

3.1.2 Molecular Characterization of Microspecies

Standard protocols were used to isolate and sequence DNA from microspecies. The morphological data and sequencing results confirmed that specific strains belong to different genera. The collected data were submitted to GenBank (Fig. 2).

3.1.3 Phylogenetic Analysis

The 18S rRNA gene sequence was analysed against multiple sequences from GenBank using the BLASTN program. Alignment was performed with CLUSTAL W software. Distances were assessed using Kimura's two-parameter correction. Phylogenetic trees were constructed employing the neighbour-joining method with Maximum Composite Likelihood. A bootstrap analysis was carried out based on 1000 replications. All analyses were performed using the MEGA-X package.

3.2 Quantification of PHB

The PHB yield of 3.82 g is supported by the dry cell weight of algal biomass dominated by Chlorella vulgaris, which was 5.82 g L^{-1}. The PHB absorbance was measured at 235 nm, and the resulting PHB concentration was 65.8%.

3.3 Characterization of PHB

3.3.1 FTIR

Fourier transform infrared spectroscopy was employed to explore the potential interactions between PHB and corn starch. Fig. 3-5 display the FTIR spectra of composites of PHB with varying ratios of corn starch. The peak at 514.99 cm^{-1} corresponds to the strain deformations of C-O-C. The spectra depict a broad peak between 1900 and 1600 cm^{-1}, linked to the deformation of hydroxyl group vibrations, correlated with intermolecular hydrogen bonds. C-H stretching appears between 1900 and 2900 cm^{-1}, exhibiting asymmetry, while the stretching of C-C and C-O bonds occurs between 990 and 1110 cm^{-1}, forming C-O-C bonds, a finding supported by Reis *et al*. (2008). The angular deformation vibrations are noted between 1510 to 1590 cm^{-1} in conjunction with O-H bonds (Florez *et al.* 2019). The formation of new hydrogen bonds in starch composites results from disrupting polymer chains from intermolecular bonds. The lower molecular weight of plasticizer facilitates easy integration into the composite starch. The broad peak observed in the polymer composites of PHB and corn starch across various proportions shows a peak at around 1722 cm^{-1} in all composites, modifying the hydrogen bond structure in the PHB and corn starch mixtures. A similar peak was noted at 1722 cm^{-1} by Zhang and Thomas (2010). Conversely, peaks at 1290 and 1400 cm^{-1} correspond to the angular deformation of CH_3 group. Peaks between 450 and 1520 cm^{-1} are attributed to stretching of C-O-C and C-C bonds. The diminishing carbon-carbon stretching bonds demonstrate the amorphous nature of PHB and corn starch composites. The weak peak around 1599 cm^{-1} is related to crystal defects at the interface of OH groups.

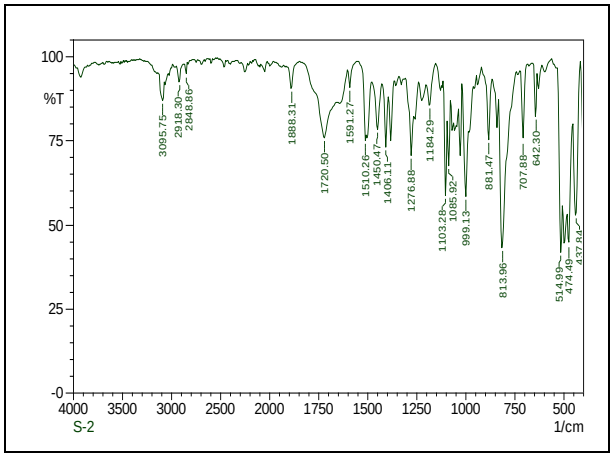


Fig. 4: FTIR spectrum in the zones of PHB (60%) and starch (40%) composite blends

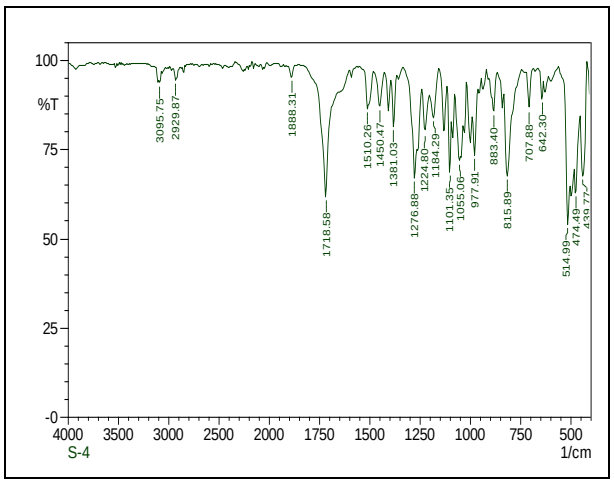


Fig. 5: FTIR spectrum in the zones of PHB (70%) and starch (30%) composite blends

3.4 SEM Analysis on PHB and Corn Starch Polymer Composites

The morphology of composite materials made from PHB and corn starch in varying blends (50/50, 60/40 and 70/30) was examined using SEM (Fig. 6 - 8). These figures illustrate homogeneous dispersion of starch and PHB. The SEM image of 50% PHB and 50% corn starch composite displays non-uniform dispersion in certain regions due to the ineffective starch reinforcement with the base matrix during casting. From the SEM image of the 60% PHB and 40% corn starch blend, it can be inferred that weaker interfacial bonding led to the formation of voids and pores in some areas. The starch did not disperse adequately due to issues with melting and agglomeration. The PHB surfaces with 40% starch appeared brittle, resulting in diminished tensile properties. Additionally, cracks were noted, contrasting with the 70% PHB and 30% cornstarch mixture, which indicates a successful homogeneous dispersion within the composite, attributed to the adequate mixing. This observation highlights that reducing corn starch while increasing the PHB content is crucial for enhancing mechanical properties. This specific composite ratio demonstrated superior tensile strength. Lai *et al.* (2006) confirmed that these results align well with previous research findings.

The ductile nature of PHB composites was enhanced by 30% corn starch, leading to increased ductility due to the observed homogeneous dispersion. This composite displayed improved grain formation and more plastic deformation due to greater ductility in comparison to those with 50/50 and 60/40 ratios that showed less plastic deformation and non-homogeneous dispersion in specific areas. In contrast, lower PHB concentrations with a high corn starch ratio resulted in reduced plastic deformation and pore formation. In other two samples the limited plastic deformation contributed to specimen failure without stretching, reflecting high brittleness.

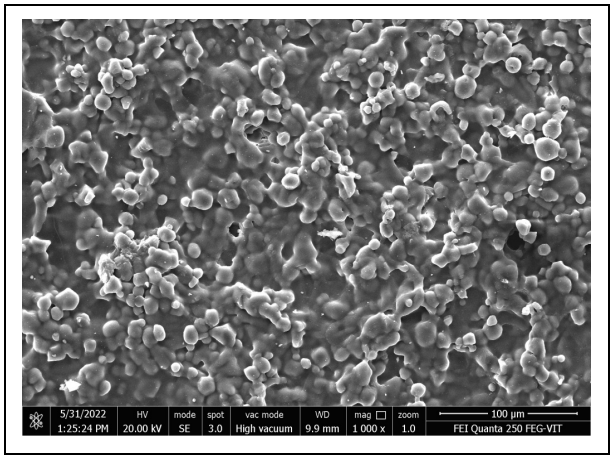


Fig. 6: SEM images of PHB and starch composite at 50/50 weight fraction

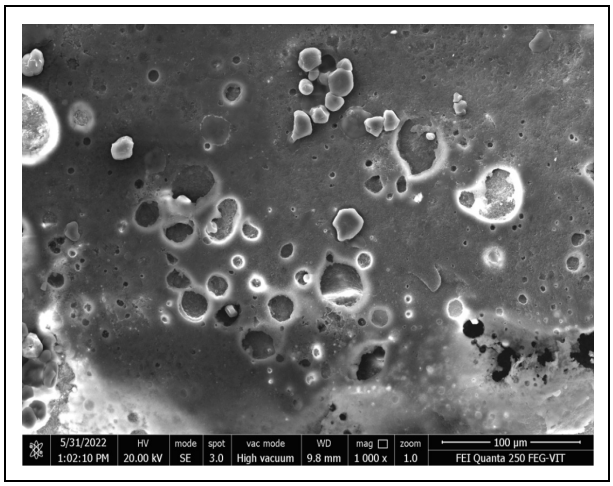


Fig. 7: SEM images of PHB and starch composite at 60/40 weight fraction

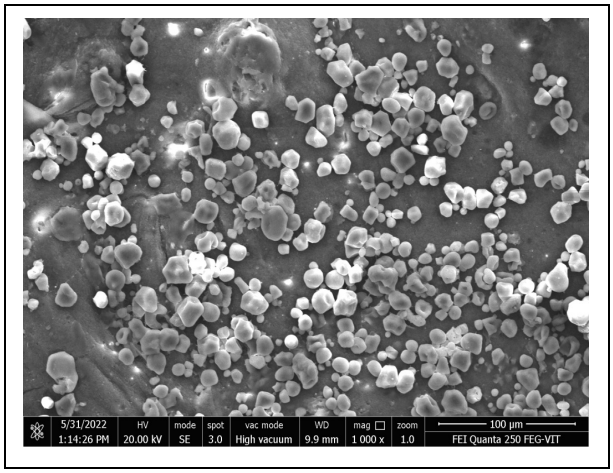


Fig. 8: SEM images of PHB and starch composite at 70/30 weight fraction

3.5 Mechanical Properties

Table 1 displays the tensile strength and elongation percentages of the composite specimens. Increase in corn starch content leads to reduced tensile strength caused by the composite's brittleness, which shows less uniform dispersion as indicated by the SEM analysis discussed previously.

Table 1. Mechanical properties of PHB and corn starch composites

S. No.	Weight Proportions of PHB and Corn Starch	Tensile Strength (MPa)	% Elongation
1	50/50	31.01 ± 0.48	3.13 ± 0.09
2	60/40	30.21 ± 0.58	3.09 ± 0.21
3	70/30	32.32 ± 0.62	3.52 ± 0.15

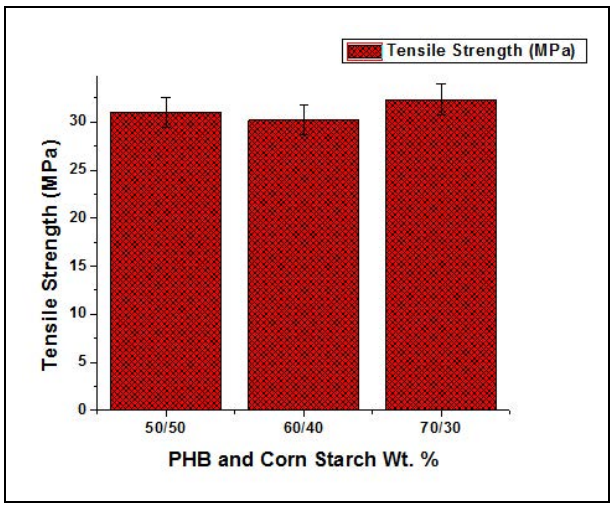


Fig. 9: Tensile strength of PHB and corn starch with different proportions

3.5.1 Tensile and Yield Strength

The tensile strength measures 31.01, while the elongation percentage is 3.13 for composite with a 50/50 ratio of PHB and corn starch. The composite with a 60% PHB and 40% corn starch ratio displayed reduced interfacial strength, evidenced by the SEM image that shows pore formation. This reduction in tensile strength likely occurs because the higher starch content in the PHB base matrix weakens the interfacial strength of the PHB-starch composites. As a result, the diminished interfacial strength obstructs the breaking of the intermetallic blend. However, adding starch to PHB at certain levels can enhance its mechanical properties. The tensile strength of the other two combinations remains lower than that of 70/30 PHB and corn starch ratio.

The lower tensile properties observed in the 50/50 and 60/40 blends reveal a decline in elongation percentages to 3.13 and 3.09, respectively, compared to the 70/30 PHB-starch composite sample. The 70/30 PHB-starch composite shows an improvement in mechanical properties driven by the interfacial conditions between the base matrix and reinforcement, along with the even dispersion of corn starch in the PHB matrix, yielding greater tensile strength and elongation percentages of 32.32 and 3.52, respectively. Fig. 9 presents the tensile strength, while Fig. 10 depicts the percentage elongation of the composite samples.

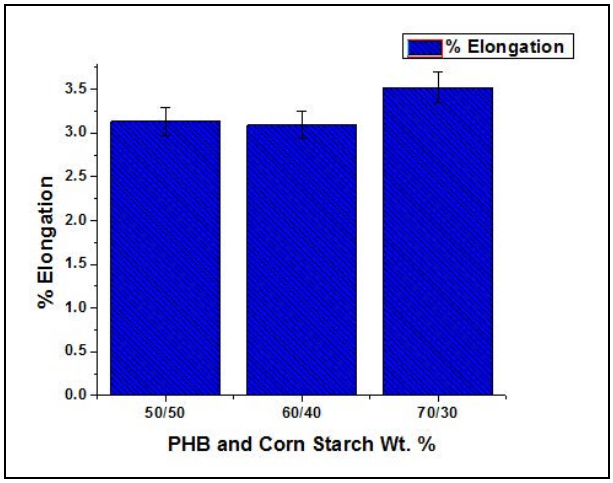


Fig. 10: Percentage elongation of PHB and corn starch with different proportions

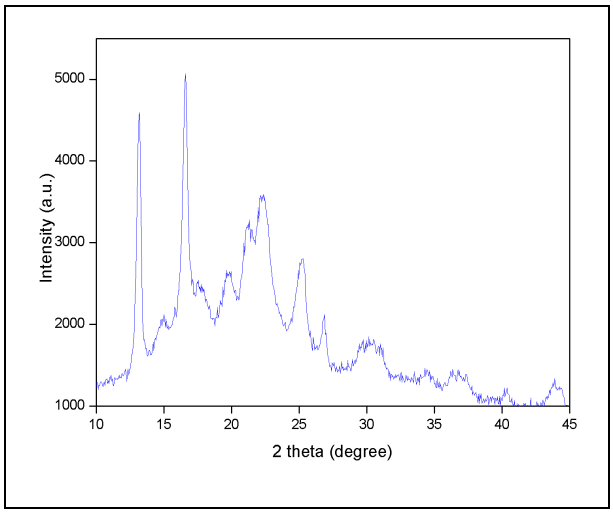


Fig. 11: XRD pattern of PHB and starch composite at 50/50 weight fraction

3.6 X-Ray Diffraction on PHB and Starch Blends

Fig. 11-13 illustrate the X-ray diffraction patterns for the composite films with PHB and corn starch in 50/50, 60/40, and 70/30 ratios. The XRD pattern of 50/50 blend showed a peak intensity of 5000 at 17.20° of 2θ. This indicates a more crystalline structure, as noted by Thiré *et al.* (2006), resulting from a higher concentration of PHB. At the same time, an increased

proportion of corn starch tends to lower the intensity. The spectrum of 60/40 blend shows two intense peaks at 17.5° and 24.5° with an intensity level around 3000, attributed to the increased concentration of PHB. The overall crystallinity decreased due to the greater starch incorporation in PHB. The 70/30 blend exhibited peaks at 13.5°, 17.8° and 24.5° of 2θ, with intensity levels between 5500 and 7000. The elevated PHB concentration coupled with a reduced corn starch fraction, enhances the crystallinity of the resulting composite materials.

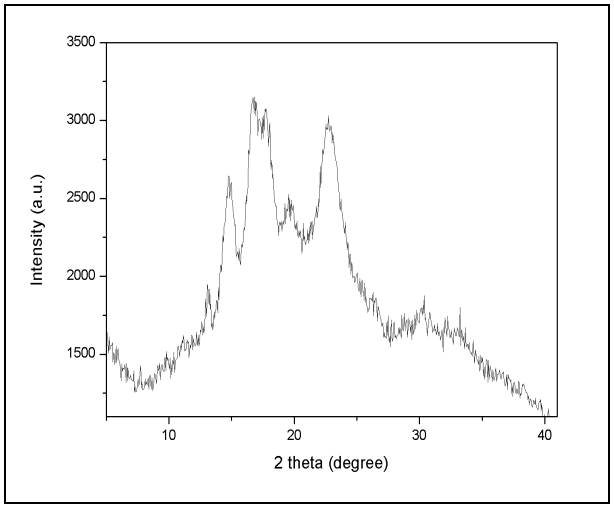


Fig. 12: XRD pattern of PHB and starch composite at 60/40 weight fraction

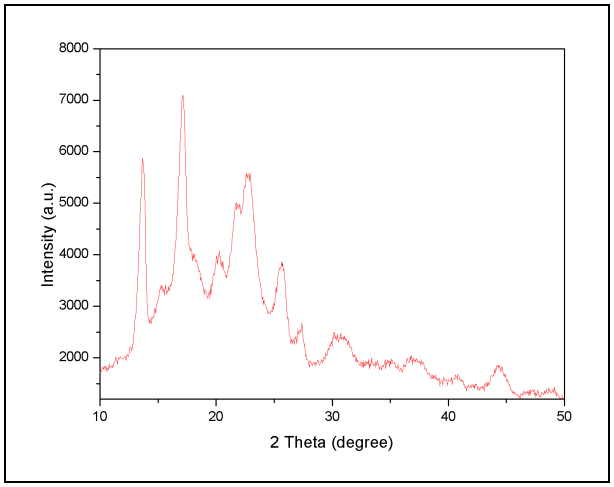


Fig. 13: XRD pattern of PHB and starch composite at 70/30 weight fraction

3.7 FESEM with EDS on PHB and Corn Starch Blends

Fig. 14-16 present the results of FESEM and EDS studies of the PHB-corn starch blends. The 50/50 PHB and corn starch blend had oxide and carbon levels at 51.6 and 48.4, respectively, with well-dispersed PHB and corn starch. The 60/40 sample showed 61.2 and 38.8 wt % of carbon and oxide levels, respectively. In this sample, some pores are formed and distinctly visible. The 70/30 sample displayed 53.1 and 46.9 wt% of carbon and oxide values, respectively.

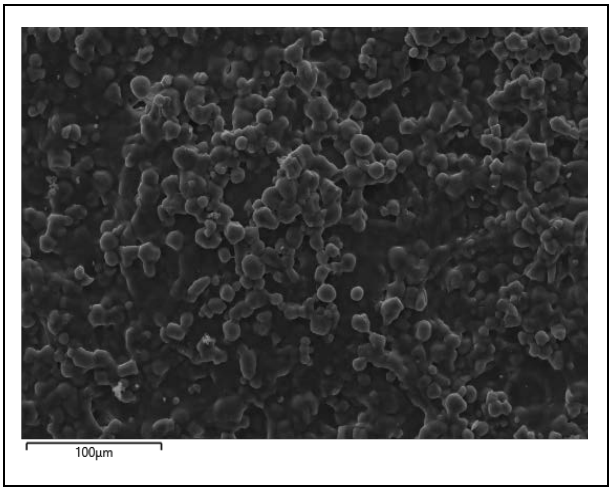


Fig. 14: (a) FESEM of PHB and starch composite at 50/50 weight fraction

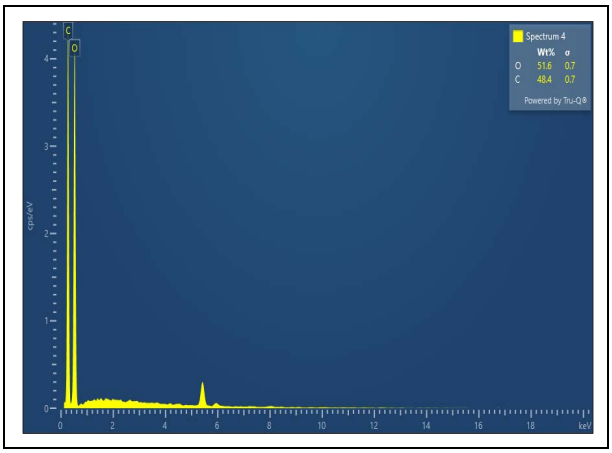


Fig. 14: (b) EDS of PHB and starch composite at 50/50 weight fraction

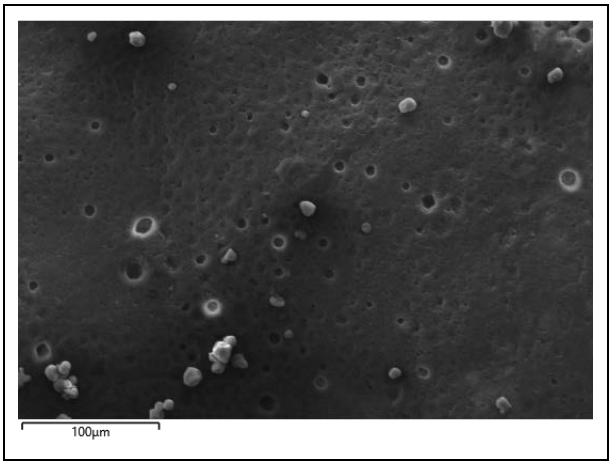


Fig. 15: (a) FESEM of PHB and starch composite at 60/40 weight fraction

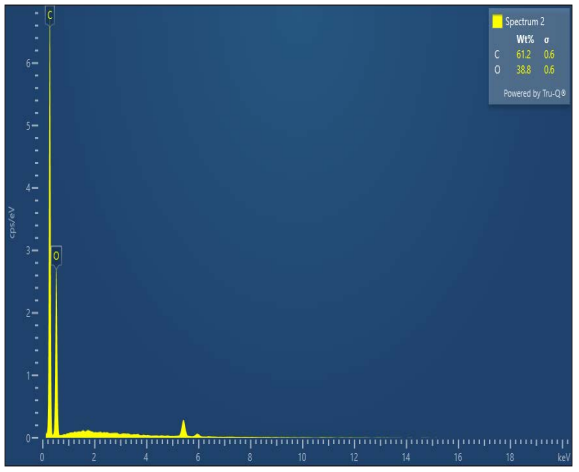


Fig. 15: (b) EDS of PHB and starch composite at 60/40 weight fraction

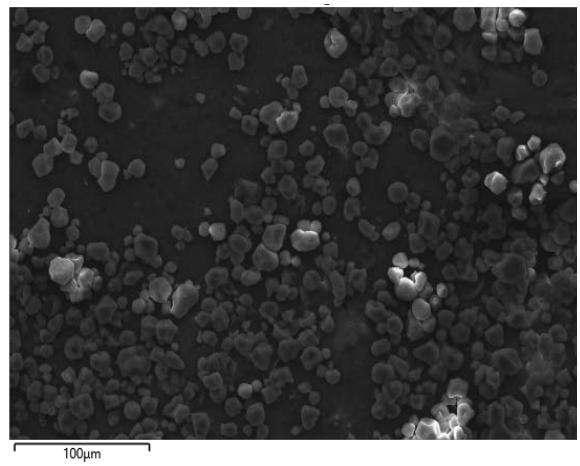


Fig. 16: (a) FESEM of PHB and starch composite at 70/30 weight fraction

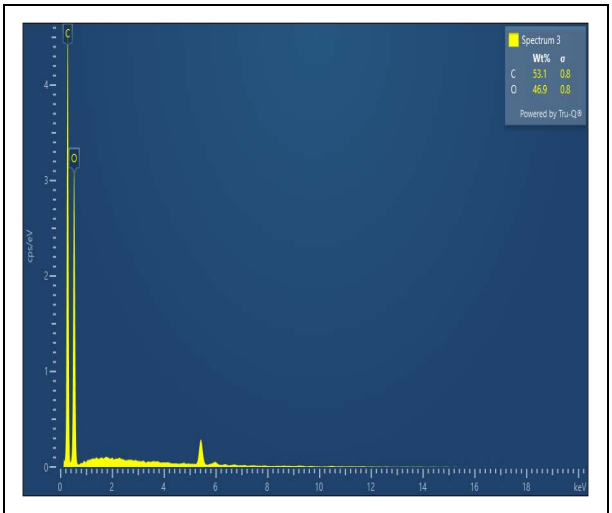


Fig. 16: (b) EDS of PHB and starch composite at 70/30 weight fraction

3.8 Biodegradation of PHB and Starch Blends

Biodegradation analysis is a critical indicator for assessing the decomposition rate of polymer blends. In this study, the samples were subjected to a 30-day soil burial test, with weight loss measurements recorded at 10-day intervals (Table 2, Fig. 17). All formulations demonstrated progressive degradation, with the 70/30 blend exhibiting the highest percentage of weight loss, indicating superior biodegradability.

Table 2. Soil burial test on PHB and corn starch blends

PHB / Corn Starch Blends	Weight Loss Percentage		
	10^{th} day	20^{th} day	30^{th} day
50/50	0.9	1.65	3.10
60/40	0.7	1.27	2.68
70/40	1.10	2.10	4.05

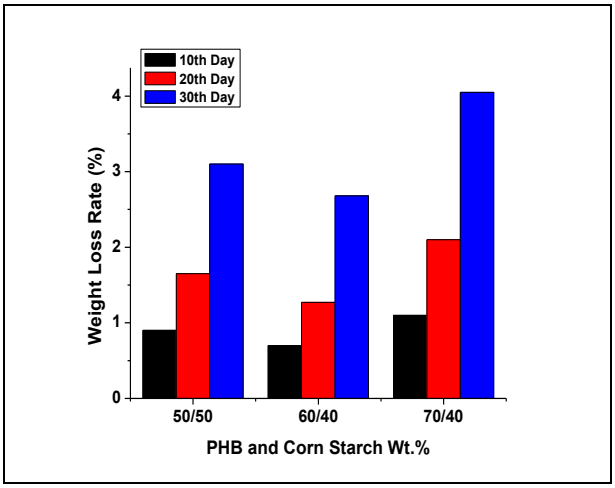


Fig. 17: Weight loss rate with various PHB and corn starch blends

4. CONCLUSION

The base matrix of PHB reinforced with corn starch is efficiently produced using the traditional casting method. Among the various blend ratios, the 70/30 mix of PHB and corn starch achieves the optimal mechanical strength and percentage elongation at 32.32 MPa and 3.52, outperforming the 50/50 (31.01 MPa and 3.13) and 60/40 (30.21 MPa and 3.09) combinations. The XRD studies further confirm that crystallinity is enhanced in the blend comprising 70% PHB and 30% corn starch. The SEM analysis of the blends, particularly those with 70/30 and 50/50 ratios, shows a uniform distribution of PHB within the starch composites, which improves interfacial strength in these samples. Additionally, FESEM and EDS validate the presence of carbon and oxide ranges on the intermetallic surface of the composites. The biodegradation tests demonstrated that the 70/30 blend displayed the highest weight loss ratio.

ACKNOWLEDGEMENT

The authors thank the CO_2 Research and Green Technologies Centre, Vellore Institute of Technology, Vellore, TN, India and the School of Civil Engineering for supporting this research. They also thank the Director of CO_2 RGTC and the management of VIT University, Vellore, TN, India for their encouragement and assistance with this work.

FUNDING

This research received no specific grant from any funding agency in the public, commercial, or not-for-profit sectors.

CONFLICTS OF INTEREST

The authors declare that there is no conflict of interest.

COPYRIGHT

This article is an open-access article distributed under the terms and conditions of the Creative Commons Attribution (CC BY) license (http://creativecommons.org/licenses/by/4.0/).

REFERENCES

Asl, M. A., Karbasi, S., Beigi, B. S., Benisi, S. Z. and Saeed, M., Polyhydroxybutyrate-starch/carbon nanotube electrospun nanocomposite: A highly potential scaffold for bone tissue engineering applications, *Int. J. Biol. Macromol.,* 223, 524–542(2022). https://doi.org/10.1016/j.ijbiomac.2022.11.023

Asl, M. A., Karbasi, S., Beigi-Boroujeni, S., Zamanlui Benisi, S. and Saeed, M., Evaluation of the effects of starch on polyhydroxybutyrate electrospun scaffolds for bone tissue engineering applications, *Int. J. Biol. Macromol.,* 191, 500–513(2021). https://doi.org/10.1016/j.ijbiomac.2021.09.078

Boura, K., Dima, A., Nigam, P. S., Panagopoulos, V., Kanellaki, M. and Koutinas, A., A critical review for advances on industrialization of immobilized cell Bioreactors: Economic evaluation on cellulose hydrolysis for PHB production, *Bioresour. Technol.,* 349, 126757(2022). https://doi.org/10.1016/j.biortech.2022.126757

Briassoulis, D., Athanasoulia, I. G. and Tserotas, P., PHB/PLA plasticized by olive oil and carvacrol solvent-cast films with optimised ductility and physical ageing stability, *Polym. Degrad. Stab.,* 200, 109958(2022). https://doi.org/10.1016/j.polymdegradstab.2022.109958

Briassoulis, D., Tserotas, P. and Athanasoulia, I.-G., Alternative optimization routes for improving the performance of poly(3-hydroxybutyrate) (PHB) based plastics, *J. Clean. Prod.,* 318, 128555(2021). https://doi.org/10.1016/j.jclepro.2021.128555

Corradini, E., Marconcini, J. M., Agnelli, J. A. M. and Mattoso, L. H. C., Thermoplastic blends of corn gluten meal/starch (CGM/Starch) and corn gluten meal/polyvinyl alcohol and corn gluten meal/poly (hydroxybutyrate-co-hydroxyvalerate) (CGM/PHB-V), *Carbohydr. Polym.,* 83(2), 959–965(2011). https://doi.org/10.1016/j.carbpol.2010.09.004

Feng, L., Yan, J., Jiang, Z., Chen, X., Li, Z., Liu, J., Qian, X., Liu, Z., Liu, G., Liu, C., Wang, Y., Hu, G., Dong, W. and Cui, Z., Characterization of polyhydroxybutyrate (PHB) synthesized by newly isolated rare actinomycetes Aquabacterium sp. A7-Y, *Int. J. Biol. Macromol.,* 232, 123366(2023). https://doi.org/10.1016/j.ijbiomac.2023.123366

Fernández, J., Saettone, P., Franchini, M.C., Villar, C.J. and Lombó, F., Antitumor bioactivity and gut microbiota modulation of polyhydroxybutyrate (PHB) in a rat animal model for colorectal cancer, *Int. J. Biol. Macromol.,* 203, 638–649(2022). https://doi.org/10.1016/j.ijbiomac.2022.01.112

Florez, J. P., Fazeli, M. and Simão, R.A., Preparation and characterization of thermoplastic starch composite reinforced by plasma-treated poly (hydroxybutyrate) PHB, *Int. J. Biol. Macromol.,* 123, 609–621(2019). https://doi.org/10.1016/j.ijbiomac.2018.11.070

Kervran, M., Vagner, C., Cochez, M., Ponçot, M., Saeb, M. R. and Vahabi, H., Thermal degradation of polylactic acid (PLA)/polyhydroxybutyrate (PHB) blends: A systematic review, *Polym. Degrad. Stab.,* 201, 109995(2022). https://doi.org/10.1016/j.polymdegradstab.2022.109995

Lai, S. M., Don, T. M. and Huang, Y. C., Preparation and properties of biodegradable thermoplastic starch/poly(hydroxy butyrate) blends, *J. Appl. Polym. Sci.,* 100(3), 2371–2379(2006). https://doi.org/10.1002/app.23085

Lee, J., Park, H. J., Moon, M., Lee, J. S. and Min, K., Recent progress and challenges in microbial polyhydroxybutyrate (PHB) production from CO2 as a sustainable feedstock: A state-of-the-art review, *Bioresour. Technol.,* 339, 125616(2021). https://doi.org/10.1016/j.biortech.2021.125616

Lin, Y., Guan, Y., Dong, X., Ma, Y., Wang, X., Leng, Y., Wu, F., Ye, J. W. and Chen, G. Q., Engineering Halomonas bluephagenesis as a chassis for bioproduction from starch, *Metab. Eng.,* 64, 134–145(2021). https://doi.org/10.1016/j.ymben.2021.01.014

Ma, P., Xu, P., Chen, M., Dong, W., Cai, X., Schmit, P., Spoelstra, A. B. and Lemstra, P.J., Structure–property relationships of reactively compatibilized PHB/EVA/starch blends, *Carbohydr. Polym.,* 108, 299–306(2014). https://doi.org/10.1016/j.carbpol.2014.02.058

Moreira, J. B., Kuntzler, S. G., Vaz, B. da S., da Silva, C. K., Costa, J. A. V. and de Morais, M. G. Polyhydroxybutyrate (PHB)-based blends and composites. Biodegradable Polymers, *Blends. Compos.,* 389–413 (2022). https://doi.org/10.1016/B978-0-12-823791-5.00007-7

Movahedi, M. and Karbasi, S., Electrospun halloysite nanotube loaded polyhydroxybutyrate-starch fibers for cartilage tissue engineering, *Int. J. Biol. Macromol.,* 214, 301–311(2022). https://doi.org/10.1016/j.ijbiomac.2022.06.072

Nygaard, D., Yashchuk, O., Noseda, D. G., Araoz, B. and Hermida, É. B., Improved fermentation strategies in a bioreactor for enhancing poly(3-hydroxybutyrate) (PHB) production by wild type Cupriavidus necator from fructose, *Heliyon.,* 7(1), e05979(2021). https://doi.org/10.1016/j.heliyon.2021.e05979

Park, S. L., Cho, J. Y., Choi, T. R., Song, H. S., Bhatia, S. K., Gurav, R., Park, S. H., Park, K., Joo, J. C., Hwang, S.Y. and Yang, Y. H., Improvement of polyhydroxybutyrate (PHB) plate-based screening method for PHB degrading bacteria using cell-grown amorphous PHB and recovered by sodium dodecyl sulfate (SDS), *Int. J. Biol. Macromol.,* 177, 413–421(2021). https://doi.org/10.1016/j.ijbiomac.2021.02.098

Plavec, R., Hlaváčiková, S., Omaníková, L., Feranc, J., Vanovčanová, Z., Tomanová, K., Bočkaj, J., Kruželák, J., Medlenová, E., Gálisová, I., Danišová, L., Přikryl, R., Figalla, S., Melčová, V. and Alexy, P., Recycling possibilities of bioplastics based on PLA/PHB blends, *Polym. Test.,* 92, 106880(2020). https://doi.org/10.1016/j.polymertesting.2020.106880

Reis, K. C., Pereira, J., Smith, A. C., Carvalho, C. W. P., Wellner, N. and Yakimets, I., Characterization of polyhydroxybutyrate-hydroxyvalerate (PHB-HV)/maize starch blend films, *J. Food. Eng.,* 89(4), 361–369(2008). https://doi.org/10.1016/j.jfoodeng.2008.04.022

Saratale, R. G., Cho, S. K., Saratale, G. D., Ghodake, G. S., Bharagava, R. N., Kim, D. S., Nair, S. and Shin, H. S., Efficient bioconversion of sugarcane bagasse into polyhydroxybutyrate (PHB) by Lysinibacillus sp. and its characterization, *Bioresour. Technol.,* 324, 124673(2021). https://doi.org/10.1016/j.biortech.2021.124673

Sirohi, R., Sustainable utilization of food waste: Production and characterization of polyhydroxybutyrate (PHB) from damaged wheat grains, *Environ. Technol. Innov.,* 23, 101715(2021). https://doi.org/10.1016/j.eti.2021.101715

Sirohi, R., Prakash, P. J., Kumar Gaur, V., Gnansounou, E. and Sindhu, R., Critical overview of biomass feedstocks as sustainable substrates for the production of polyhydroxybutyrate (PHB), *Bioresour. Technol.,* 311, 123536(2020). https://doi.org/10.1016/j.biortech.2020.123536

Song, Y., Matsumoto, K., Tanaka, T., Kondo, A. and Taguchi, S., Single-step production of polyhydroxybutyrate from starch by using α-amylase cell-surface displaying system of Corynebacterium glutamicum, *J. Biosci. Bioeng.,* 115(1), 12–14(2013). https://doi.org/10.1016/j.jbiosc.2012.08.004

Thiré, R. M. S. M., Ribeiro, T. A. A. and Andrade, C. T., Effect of starch addition on compression-molded poly(3-hydroxybutyrate)/starch blends, *J. Appl. Polym. Sci.,* 100(6), 4338–4347(2006). https://doi.org/10.1002/app.23215

Tian, L., Li, H., Song, X., Ma, L. and Li, Z. J., Production of polyhydroxyalkanoates by a novel strain of Photobacterium using soybean oil and corn starch, *J. Environ. Chem. Eng.,* 10(5), 108342(2022). https://doi.org/10.1016/j.jece.2022.108342

Zhang, G., Xie, W. and Wu, D., Selective localization of starch nanocrystals in the biodegradable nanocomposites probed by crystallization temperatures, *Carbohydr. Polym.,* 227, 115341(2020). https://doi.org/10.1016/j.carbpol.2019.115341

Zhang, M. and Thomas, N. L., Preparation and properties of polyhydroxybutyrate blended with different types of starch, *J. Appl. Polym. Sci.,* 116(2), 688–694(2010). https://doi.org/10.1002/app.30991

Zoghbi, L., Argeiti, C., Skliros, D., Flemetakis, E., Koutinas, A., Pateraki, C. and Ladakis, D., Circular PHB production via Paraburkholderia sacchari cultures using degradation monomers from PHB-based post-consumer bioplastics as carbon sources, *Biochem. Eng. J.,* 191, 108808(2023). https://doi.org/10.1016/j.bej.2023.108808